Redesign of the F-35 Horizontal Stabiliser Leading Edge

Inés R. Pastor, Fraizer F. Cardoso, Mads G. Poulsen, Robin K. Olesen, Martin R. Laursen

Department of Materials and Production, Aalborg University
Fibigerstraede 16, DK-9220 Aalborg East, Denmark
Email: {iruiz16,fcardo16,mgpo13,rkol13,mrla13}@student.aau.dk
Web page: http://www.mechman.m-tech.aau.dk/

Abstract

This paper concerns structural redesign and manufacturing considerations for the Leading Edge (LE) for the F-35 horizontal stabiliser. The leading edge is manufactured at TERMA and consists of five individual parts, which are glued together in a secondary bonding operation. This bonding operation is a very labour intensive and increases the cost of the component considerably. It is expected by TERMA that redesigning the leading edge to a single component to be produced using a 'single shot' manufacturing technique will lead to a cost saving of approximately 50%.

The objective of this work is therefore to analyse the existing LE using advanced FE-software to evaluate stresses and failure indices throughout the structure and evaluate the influence that the new manufacturing process will have on the structure. The second objective is then to optimize the composite layup and core material in consideration of demands, set forward by TERMA.
The approach includes an estimation of the static design loads for the horizontal stabilizer as well as a structural analysis on an approximated model of this structure. Results are then used for the subsequent analysis of the leading edge.
In addition to this, an investigation of the double sided mold manufacturing process is done by the use of CFD-software and experimental testing, in order to evaluate whether the single shot LE is obtainable.

Keywords: Composite Materials, Aeroplane Design, Computational Fluid Dynamics (CFD), Finite Element Analysis (FEA), Experimental test

1. Introduction

This paper concerns the structural analysis and optimization of the Leading Edge (LE) for the F-35 fighter jet as well as the investigation and design of double sided mold manufacturing of the spar in the LE.

The LE is produced by TERMA A/S under contract of Lockheed Martin. It is a part of F-35 horizontal stabiliser, shown in Fig. 1, that enables the aircraft to manoeuvre.

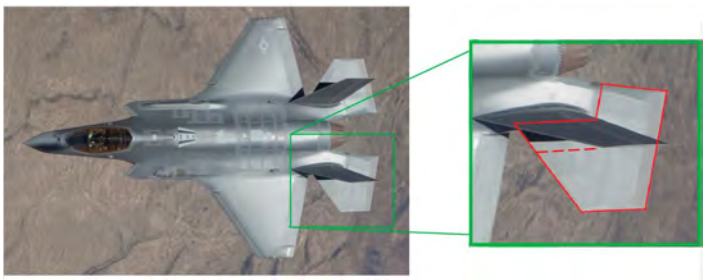

Fig. 1 F-35 from above.

The LE consists of 4 carbon fibre parts and a central honeycomb core material. It is produced through a series of steps and finally glued together in a secondary bonding operation. The current manufacturing process is therefore very labour intensive which increases the cost of the component considerably. TERMA has therefore shown interest in investigating whether or not the LE can be produced in a single-shot operation and what effects this will have on the structural performance of the LE. TERMA has estimated that redesigning the LE to be produced through a single shot manufacturing technique can lead to a cost saving of approximately 50%.
It has already been established by TERMA, that a single shot manufacturing process will require a double sided mold instead of the current auto-clave molding technique.

The objective of this work is therefore to analyse the existing LE using advanced FE-software to evaluate stresses and failure indices throughout the structure, in order to evaluate the influence that the new manufacturing process will have on the structural behaviour. The second objective is to optimize the layup and core material in consideration of demands to minimize displacements, while retaining acceptable stress levels and failure indices. In addition to this, an investigation of the double sided mold manufacturing process is done by using CFD and experimental testing, in order to evaluate whether the LE can be produced in single shot. [1]

2. Demands

The demands for a LE produced in a single shot operation are as follows:

1) Identical geometrical dimensions.
2) No failure of skin nor core.
3) Manufacturing in single shot.
4) Resin filling time of maximum 30 minutes.
5) Solid core material.
6) Identical or lower core density than PMI-foam 150 kg/m^3.

Note: 5) A solid surface is needed, otherwise the resin will flood the voids in the core.

3. Geometry and Material Properties

The geometry of the horizontal stabiliser and the LE can be seen in Fig. 2.

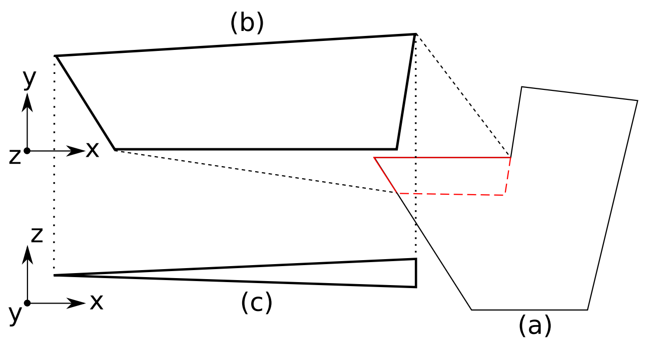

Fig. 2 (a) horizontal stabiliser, (b) leading edge, and (c) aerofoil (cross-sectional shape) of the leading edge. Coordinate systems denote the principal directions.

Material properties are listed in Tab. I. Aluminium is not included in the leading edge model, but used a reference material for carbon fibre in the finite element analysis.

	Aluminium (T7075-T6)	**Carbon Epoxy (T650-35 PW)**
E_1	65.6 GPa	71 GPa
E_2	65.6 GPa	71 GPa
G_{12}	5.5 GPa	27 GPa
X_t	646 MPa	482 MPa
X_c	638 MPa	476 MPa
Y_t	646 MPa	469 MPa
Y_c	648 MPa	496 MPa
S	103 MPa	-

Tab. I Material properties of skin material obtained from ESAcomp Databank.

4. Loads

As the actual load and airflow on the leading edge is unknown due to restrictions, the loading is obtained by first analysing the entire horizontal stabiliser using an estimation of the loading situation. This load is applied as a simplified evenly distributed pressure as illustrated in Fig. 3. This pressure has been calculated

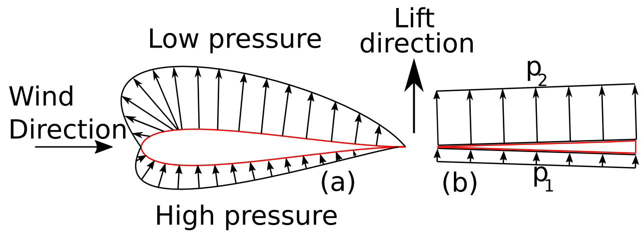

Fig. 3 Evenly distributed pressure on the plane.

by estimation of the gravitational pull on the total mass of the plane (22,680 kg) multiplied by the maximum 9 G's, that the plane can maintain during a manoeuvre. Converted to newton this gives a total force of $2 \cdot 10^6$ N. With total wing area at $42.7\ m^2$ the average pressure yields $4.7 \cdot 10^4$ Pa. The pressure load has been separated between the upper and lower surface to represent an actual load situation such that $p_1 = 1 \cdot 10^4$ Pa and $p_2 = -3.7 \cdot 10^4$ Pa, which is a distribution of approximately 20 and 80 percent respectively.

4.1 Leading Edge Component

The Leading Edge is made with face sheets of carbon fibre and honeycomb as core material. The goal is to make the construction in single shot, meaning that all components in the leading edge will be manufactured in one process.

5. Structural Analysis

The approach for the structural analysis is first to obtain displacements on the entire horizontal stabiliser that can then be applied as boundary conditions to the detailed model of the leading edge, as illustrated in Fig. 4. The detailed model incorporates the composite layup throughout the LE as well as geometric details, excluded from the stabiliser analysis. The analysis approach is consequently not an ordinary sub-modelling strategy, since the detailed geometry of LE is not implemented in the model of the stabiliser wing. The objective of the analysis is to determine stresses and failure indices (FI) throughout the leading edge. The model is subsequently utilized for optimisation of the composite layup, with the objective to lower the maximum out-of plane displacement while still maintaining acceptable stress levels and failure indices. The analyses have been performed using ABAQUS and ANSYS FE-software.

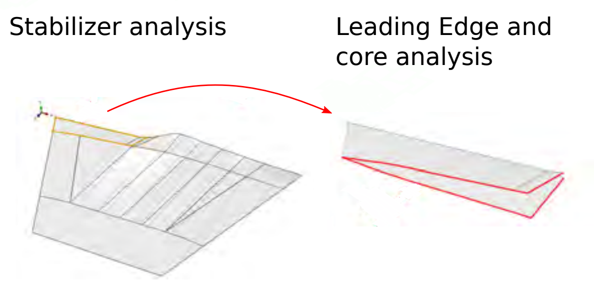

Fig. 4 Illustration of modelling approach.

5.1 Stabilizer analysis

The geometrical outline of the horizontal stabiliser, which is illustrated in Fig. 5, is obtained using publicly available information. Since actual data on the location and dimension of the internal I-beam spars has not been available, the model is based on an illustrated view of the F-35, shown in Fig. 1.

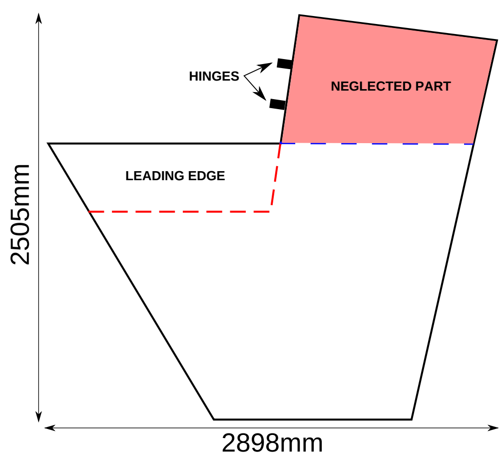

Fig. 5 Geometrical outline of the entire stabiliser wing.

The spar material is assumed to be aluminium, as this is commonly used for aerospace structures. Furthermore the model is simplified so that a part of the stabiliser is neglected from the analysis as illustrated in Fig. 5. This means that instead of being fixed at the hinges, that attach the stabilizer to the plane, the wing is fixed/clamped along the red edges shown in Fig. 6.

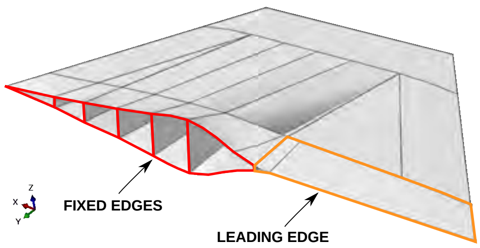

Fig. 6 FE-model of stabiliser wing using shell elements.

The FE-model is made with shell elements which allows for a simple model that is computationally inexpensive compared to solid elements. The use of shell elements has also made it easy to model the layered Carbon-Epoxy skins and the aluminium spars. The drawback to shell elements is that transverse shear stresses (σ_{13} and σ_{23}) are not accounted for, but since these stresses typically are of small magnitude [2], shell elements have been considered the best choice.

The model does not include a core inside the wing edges, which has made it necessary to constrain the skins on these sections in order to represent the core. This is done by using a surface-to-surface tie constraint that prohibits points on opposite surfaces to move relatively to one another, by locking certain DOF in the nodes. In effect the tie constraint imitates the function of a core material in a sandwich structure and basically serves to maintain the surface skins at a fixed distance away from each other in order to gain a high second order moment of area. This of course means that the stiffness of the core is not directly incorporated in the model. Additionally the composite spar that is situated inside the leading edge was not included, which has also affected the stiffness of the model.

The validity of the model and analysis is evaluated by inspecting the out-of-plane displacement results. A contour plot of these displacements is shown in Fig. 7. The maximum deflection of the horizontal stabiliser was of 21.5 mm at the tip as expected. Data regarding the deflection of an actual F-35 wing is not accessible, but the magnitude of the deflections is deemed realistic and the analysis considered sufficiently valid for the purpose of this work.

Displacement values along the interface of the leading

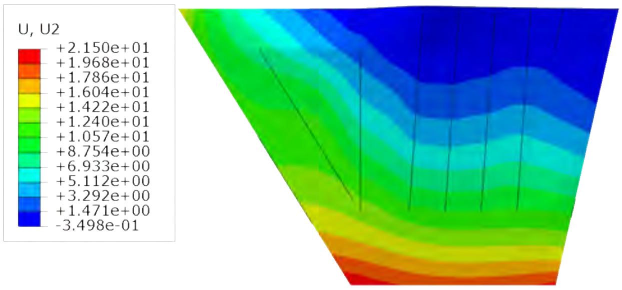

Fig. 7 Contour plot of Y-displacements on the horizontal stabiliser.

edge were then probed along the interface path and exported for later use in the leading edge analysis.

5.2 Leading edge analysis

The model of the LE is made in Abaqus. It should be noted that the original leading edge is not symmetric about the XY-plane. The model is based upon shell elements as this is the optimal approach for this analysis. This is due to the fact that primarily in-plane stresses are relevant for the evaluation of the sandwich structure whereas the out-of-plane shear stresses are non-essential. This also helps to ease modelling and to minimize computational time when performing the analysis.
Due to modelling issues the core is neglected from the leading edge model. Instead the stresses in the core and the effect of changing core material has been evaluated in a separate analysis, see section 5.4. The core is replaced with tie constraints in the leading edge model as it was done in the analysis of the horizontal stabiliser.

The boundary conditions are defined along the edges, shown in Fig. 8, using equations formulated by interpolation of the displacements exported from the analysis of the horizontal stabiliser. The pressure load, which is subjected to the stabiliser, is also applied to the leading edge.

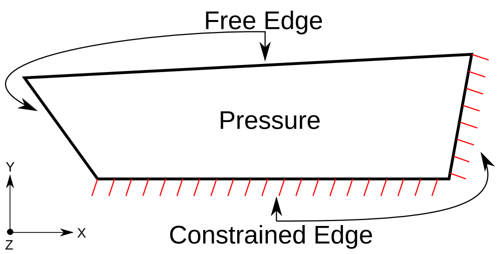

Fig. 8 Illustration of leading edge with displacement constraints, marked with red.

5.3 Results

Evaluation of the results is conducted with the objective to asses the validity of the analysis and to check whether the structure will withstand the applied loads.

Verification

The maximum deflection of the leading edge is 16.74 mm, which fits the maximum deflection of the stabilizer analysis of 16.58 mm, the difference being $< 1\%$. On basis of this it is concluded that the modelling approach for loading the LE has been sufficient for the purpose of this work. This leads to the conclusion that the analysis is sufficiently accurate to be used for structural evaluation of the LE and subsequent optimization of the structure.

When evaluating the stress levels throughout the structure, see Fig. 9, it is obvious that a stress singularity is present at the edge where the boundary conditions are defined. A convergence study using mesh refinement around this area has supported this conclusion.

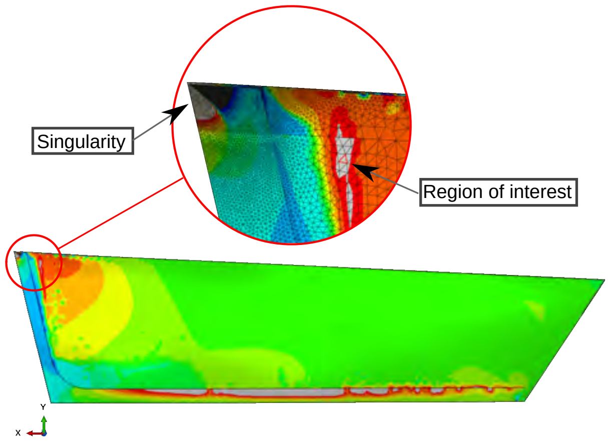

Fig. 9 Contour plot of Max. In-plane absolute principal stresses.

Failure evaluation

The purpose of the failure evaluation is to compare and discuss the results and establish a tool for estimating fibre failure in the LE.
By neglecting values in the vicinity of the spar, a region of interest is identified on the lower skin, as shown in Fig. 9. Multiple failure criteria are used to investigate through-the-thickness FI, as plotted in Fig. 10. Max. stress- strain criteria is chosen due to is simplicity it evaluates each quantity individual. Tsai-Hill is chosen since it is the simple criteria for biaxial loading based on limit of linear elastic behaviour, similar of Von-Mises yield criteria, but for a orthotropic material. Tsai-Wu is chosen as it involves higher order terms which improves

the correlation between prediction and experimental data. Tsai-Hill can be dangerous to use of the material of compression and tension are very different [3].

Multiply criteria are chosen in order to investigate he difference of their failure prediction.

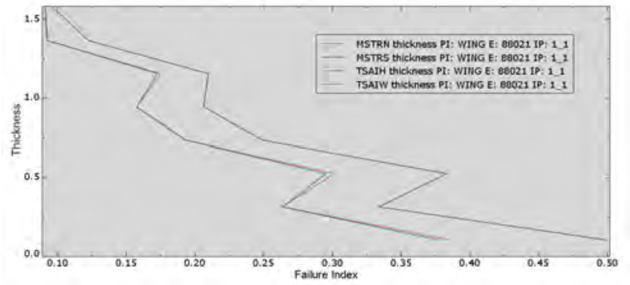

Fig. 10 Plot of through-the-thickness failure indices in element 88021.

The failure indices for the inner and outer plies are listed in Tab. II:

Failure Criteria	**FI(0mm)**	**FI(1.68 mm)**
Max Stress	0.375	0.08
Max Strain	0.385	0.08
Tsai-Hill	0.50	0.09
Tsai-Wu	0.50	0.09

Tab. II Failure Indices at inner and outer ply.

By consideration of the bi-axial stress situation ($\sigma_{11} =$ 260MPa, $\sigma_{22} = -120$MPa) in the structure, Tsai-Hill and Tsai-Wu chosen as the optimum failure criteria, as the criteria incorporates multiple failure modes in bi-axial loading. Tsai-Wu is known to underestimate the structural damage in compression-compression situations by a factor of 3, [4], but as the investigation has shown only tension-compression stress fields, the criteria is considered the proper tool for estimating failure in this particular load case.
The difference in material tension and compression, making it safe to use Tsai-Hill as well. No difference is found between Tsai-Wu and Tsai-Hill despite higher order terms incorporated in Tsai-Wu. It is assumed that the reason might be that Tsai-Wu and Tsai-Hill predicts the same failure index, as Abaqus does not include out of plane shear stresses for shell elements, meaning $\tau_{13} = \tau_{23} = 0$.

Tsai-Wu is known to underestimate the structural damage in compression-compression situations by a factor of 3, [4], but as the investigation has shown only tension-compression stress fields, the criteria is considered the proper tool for estimating failure in this particular load case.
On basis of this, it is concluded that the structure will withstand the applied loads as the failure index is of $0.5 < 1$ from Tsai-Hill and Tsai-Wu, thus complying with demand 2.
The incorporation of the core material would the found results. Further work, which incorporates the core into the model, should therefore be conducted in order to improve the accuracy of the analysis.

5.4 Core Analysis

Due to disclosure agreement honeycomb material and shear properties of the substitute material left for comparison are not provided here.
With the single shot manufacturing the honeycomb core material needs to be exchanged with a solid material to avoid getting the structure filled up with resin during injection.
Due to problems with the use of shell elements and solid element in Abaqus, a model is done in ANSYS using solid model and identical boundary conditions, to obtain stresses in the core thickness. The original skin (T650) is replaced by aluminium, as it resemble stiffness of a quasi-isotropic layup for T650, which can not be applied to a solid model. The difference in stiffness is 5% by comparing values of Tab. I. As failure between skin and core is no longer valid when using aluminium skins, the failure the sandwich structure core is narrowed down to failure in shear. The failure criteria becomes maximum shear stress:

$$max\left(\frac{\tau_{31}}{R}, \frac{\tau_{23}}{Q}\right) \leq 1 \tag{1}$$

where R and Q are the stress limits of the corresponding shear stress directions. The analysis shows that single of the two current honeycomb material fails in shear. The remaining substituted materials of balsa wood and PMI-foam, did not fail in the analysis. All materials succeed to comply with demand a, 5 and 6. As TERMA has not specified a demand regarding deflection, choosing a material with low stiffness would not be a concern thus the light material of PMI-foam at 71 kg/m^3 is suggested to replace the original honeycomb material.

6. Optimisation

Optimisation is utilized to obtain an optimum structural design, regarding either minimising weight, stress and strain, deflection by maximising stiffness, or a combination of these. Weight is often the objective in aerostructures [3], since it will allow the plane to carry more load, whereas the focus of this project is on

maximising stiffness w.r.t. fibre orientation.
The subject to minimise or maximise is referred to as the objective function or cost function f. The limits of the optimisation problem are called constraints, which can both be equality h and inequality g. The design variables are denoted as a vector $\boldsymbol{x}$.
The general model of constrained non linear optimisation problem (NLP) is written as [5]

$$\text{Minimise:} \qquad f(\boldsymbol{x}) \tag{2}$$

$$\text{Subjected to:} \qquad h_j(\boldsymbol{x}) = 0; \qquad j = 1, ..., p \tag{3}$$

$$g_i(\boldsymbol{x}) \leq 0; \qquad i = 1, ..., m \tag{4}$$

6.1 Formulation of Problem

For this work the objective function has been represented by the displacement minimisation, which directly refers to the maximisation of stiffness.
The number of design variables are quite large, leaving a comprehensive problem. The variables are narrowed down by demand 1 from TERMA, concerning the shape and material of the skins (Material, Ply thickness, Number of plies, Geometry).
Leaving only the fibre orientation and section division as the inequality constraints ($g_i(x)$) for the problem, setting the boundaries $0° - 45°$.

6.2 Sections for Optimisation

Since the principal directions are found to vary over the entire structure, it is chosen to split the geometry into main sections for the optimisation problem following the layup sections, this can be seen in Fig. 11. Each section then has an average principal stress direction.

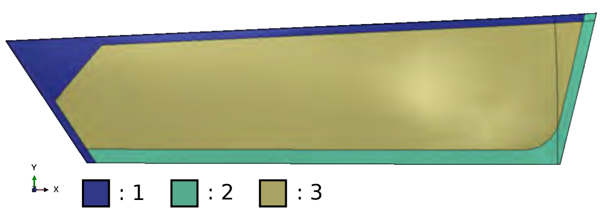

Fig. 11 FE-model of stabiliser wing using shell elements.

6.3 Direction of Principal Stress

The load carrying capacity of a composite is much higher in the fiber direction, as a result fibers are oriented parallel to the largest stress direction. Meaning that the preferable orientation is $0°$ for bending and tension load cases and $\pm 45°$ for shear and torsion. For more complicated structures and load cases, as the leading edge, the use of fibres can be oriented in the principal stress direction. The principal stress direction is determined from an eigenvalue problem by equation 5:

$$(\sigma_{ij} - \sigma\delta_{ij})v_j = 0 \tag{5}$$

where v_j is the principal direction of stress to the corresponding principal stresses σ.
As shell elements are used, the principal directions will stay in plane, while the out of plane stress $\sigma_{33} = 0$, and the directions is easily be found by visualisation using an ABAQUS plot. Changing the layup of the fibres leads to v_j changes as well, thus making the problem non-convex. The problem is solved iteratively. The initial guess of fibre orientation is based on a skin of an isotropic material, in this case aluminium due to its resemblance of carbon fibre, see section 5.4. After analysing the new deflection, the fibre orientation is then changed manually until a feasible design w.r.t. stiffness is obtained. The layup is investigated further by examining the failure index.

6.4 Results

Due to disclosure agreement the results are normalized. Five layup combinations are tested for section 3 in Fig. 11 (The results are confidential and cannot be shown here), representing the upper skin of the leading edge. The displacement of leading edge is plotted for comparison in Fig. 12, holding a reference which originates from the original layup.

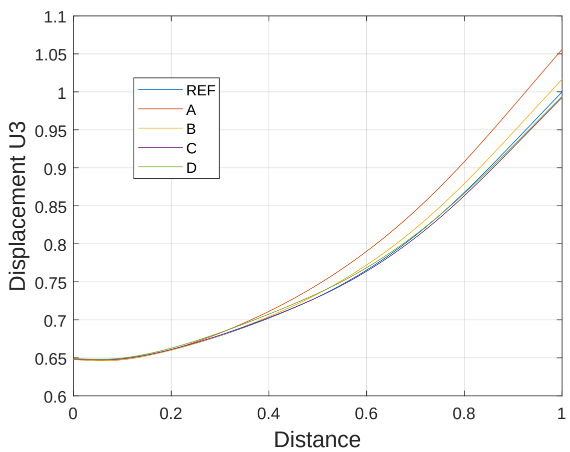

Fig. 12 Displacement of leading edge, with different layups for section 3.

Based on the particular load case found in section 5, layup (C) yields the best result. Although it only minimised the maximum displacement by 0.7%, the layup is preserved and also applied on lower skin section. Layup (G) from Fig. 13 improves the maximum displacement further with a result of 3.5%, compared to the reference.

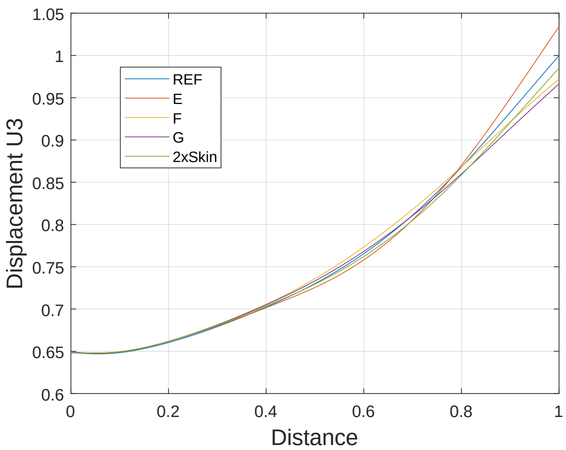

Fig. 13 Displacement of leading edge, with different layups for section 2.

Tsai-Wu failure criteria is used to verify, that the optimised layup, will withstand the load case. As it shows in Fig. 14, FI of Tsai-Wu has increased from earlier analysis on same element.

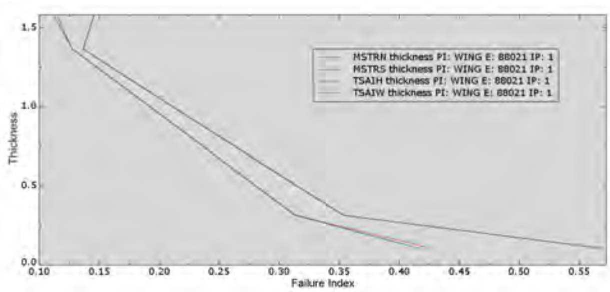

Fig. 14 Failure criteria for optimised layup, refer to same element as used earlier.

The difference in FI can be explained, since the object has been to minimise the maximum displacement, which implicit results in a higher stiffness. From the governing equation from FEA:

$$[K]\{D\} = \{R\} \tag{6}$$

it can seen that applying the same displacement $\{D\}$ to a stiffer structure $[K]$, will results in higher forces $\{R\}$ resulting in increased stress levels.

7. Manufacturing

For the investigation of the double sided mold manufacturing process, the focus has been laid on the composite spar, situated inside the leading edge. This is done in order to narrow down the investigation process, but it is believed that once the manufacturing process has been mastered, it can be extended to the rest of the leading edge. Currently at TERMA, the manufacturing process used is thermoforming i.e. vacuum forming which applies vacuum to give shape to the components. This process is limited by complicated geometries and involves high costs per piece. As an alternative, a process making use of a double sided mould is considered and evaluated here, as it allows for the manufacturing of the LE through a single shot manufacturing process, thus fulfilling demand 3 specified by TERMA.

7.1 Theory

The investigation of the molding process implies the use of Darcy Law theory. Darcy Law describes the motion of a fluid flowing through a porous medium. In this case, it is the resin that flows through the carbon fibres (porous medium). The Darcy Law is expressed by, [6]

$$Q = -K\frac{A}{\mu}\Delta P \tag{7}$$

Where Q is the volume flow in $[m^3/s]$, K is the permeability of the porous medium in $[m^2]$, μ is the viscosity in $[Pa \cdot s]$ and pressures are measured in $[Pa]$. The flow area A is defined by cross sectional area divided by porosity of the medium. In order to obtain the velocity of the flow, the previous expression is divided by the cross-section area, yielding:

$$v = \frac{Q}{A} = -\frac{K}{\mu}\frac{dP}{dx} \tag{8}$$

This expression is proven to be the solution for the momentum and continuity equation at any infinitesimal volume within the porous medium, hence by integration, the position of the flow at any time is obtained. As it can be seen, permeability and porosity of the carbon fibre and viscosity of the resin are critical process parameters that need to be determined through this study.

Resin flow is a crucial part of the fabrication of structural laminates, and is therefore a critical issue as the material properties depend directly on the filling of cavities within the mold. It is important to achieve a good continuous flow in order to avoid bubbles or voids within the composite.
The case of two-phase Darcy Law is studied through this

work, as air is present between carbon fibres prior to the resin injection. This makes Darcy Law to be saturation dependent and two expressions are needed in order to solve the problem - one for the resin phase (denoted with suffix w) and a second for the air phase (denoted with suffix a):

$$v_w = -\frac{K_w(S_w)}{\mu}\Delta(p_w) \quad ; \quad v_a = -\frac{K_a(S_a)}{\mu}\Delta(p_a)$$

7.2 Simulation and Experiment with Glycerol

Double sided mould manufacturing of composites involves creating a mold with the desired shape, placing the carbon fibre plies, closing the mould, injecting heated resin and finally leaving it to cure.
The first step in the investigation is to consider only a section of the spar, shown in Fig. 15.

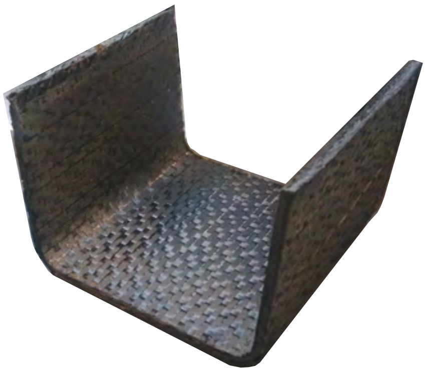

Fig. 15 Section of spar, used for evaluating manufacturing process.

A computed simulation is performed to estimate the filling time of the mold, which can then be compared to experimental data. A physical mold has therefore been fabricated for the experiments. In order to observe the resin flow through the mold, the lower part is manufactured in acrylic glass as seen in Fig. 16.

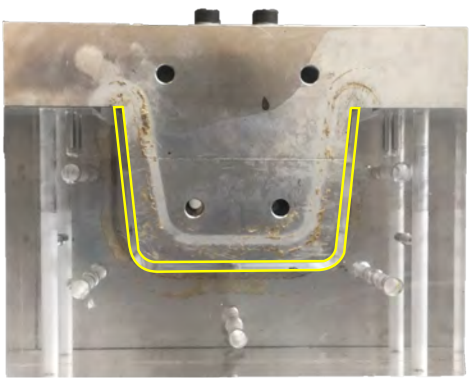

Fig. 16 Double sided mold fabricated for the experimental tests.

As the resin needs to be heated to $130°C$ to obtain a sufficiently low viscosity, another liquid is needed for the flow analysis, due to a glass transition temperature of acrylic glass of $110°C$.
The resin has a dynamic viscosity μ of $0.234\ Pa \cdot s$. A viscosity test conducted using glycerol at room temperature ($20°C$) yield a value of $0.230\ Pa \cdot s$, thus making a appropriate substitute liquid for testing.

The permeability coefficient K of the fibre material has been established through research ($2.22 \cdot 10^{-10}\ m^2$). [7], [8] and [9].

Fig. 17 shows the simulation of the filling process, made using COMSOL Multiphysics software. The colourbar represents the saturation within the filling process, where blue phase is air and red phase is glycerol. Fig. 18 shows the flow front during experimental test, performed using glycerol.

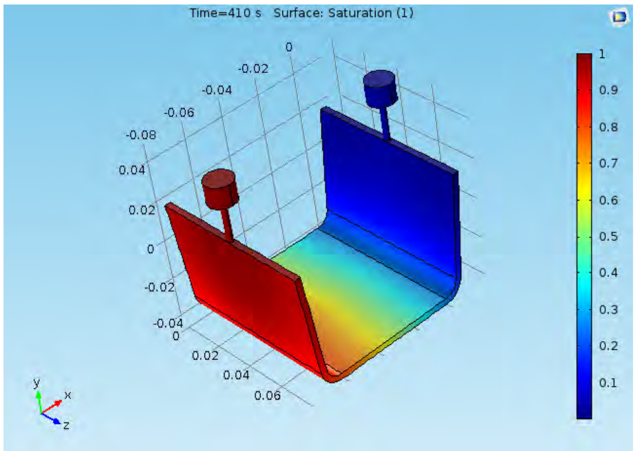

Fig. 17 Simulation of the glycerol injection made in COMSOL.

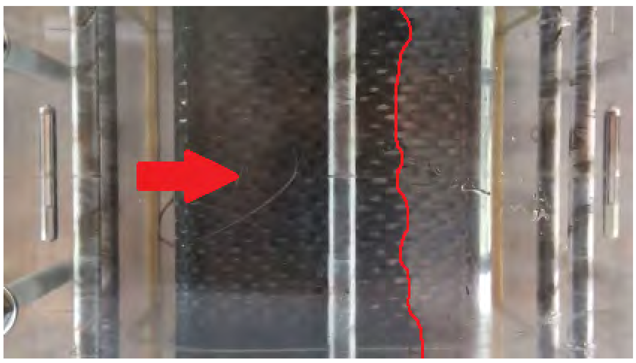

Fig. 18 Bottom view of the flow front, as seen during experiment.

In both cases, a filling time of 21 minutes is obtained applying a pressure of 3.5 Bar at the inlet and releasing the flow at atmospheric pressure in the outlet. By comparison of simulation and experimental results, the simulation is verified.

7.3 RTM Experiment at TERMA

Once it has been proven that COMSOL Multiphysics provides reliable solutions and the porosity of the plies have been established, the resin transfer molding (RTM) is investigated. A new simulation is made using properties of resin at a working temperature of 130° C. The filling time is 18 min. For the experiment, a new bottom part of the mold is manufactured in aluminium, in order for the mold to withstand the elevated temperatures. First, resin pre-impregnated plies are placed inside the mold, then the whole set is placed inside an oven and resin is injected at 130° C. Inlet and outlet pressures are kept constant. Once the mold is filled, a the curing process takes place at 180° C, to completely harden the resin and obtain the desired stiffness in the composite.

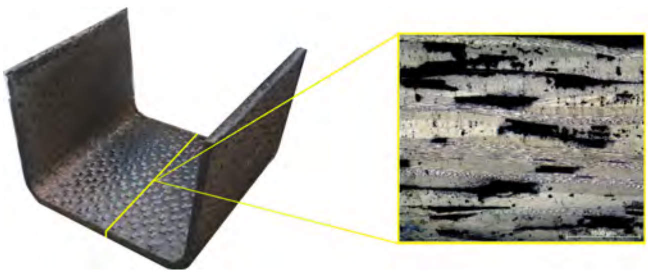

Fig. 19 Composite test specimen without resin injection, displayed with the cut through surface.

Besides from the RTM experiment, an experiment is made without resin injection, leaving the plies to cure right away. This is done to investigate the importance of resin injection.

An investigation of the quality of the composite component is conducted in order to verify the simulation. This is done by cutting out a piece from the centre of the material, as illustrated in Fig. 19, and examine it under microscope.
For the non-RTM spar, the voids are determined to make up $> 15\%$ of the material, thus making the material useless for structural members, since voids are impose as initial cracks in a structure, causing the fatigue life to be reduced dramatically.

The spar specimen, made using RTM, has a generally acceptable micro structure in most of the investigated cross section, as shown in Fig. 20. Some empty voids of the size of 500 μm (0.5 mm) are detected, occupying

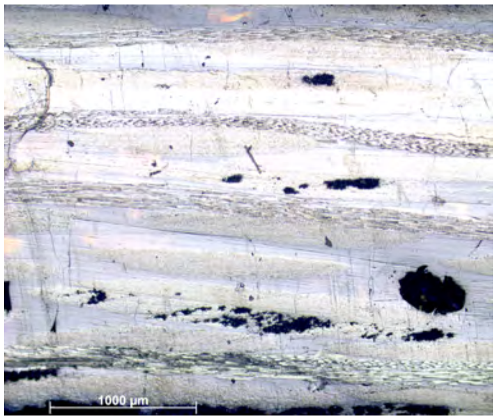

Fig. 20 Microscopic image of the section perpendicular to the resin flow of the composite spar.

about 4% of the cross-sectional area. This amount of voids exceeds the allowable amount in aircraft industry of 1% according to [10]. It is believed that these defects can be avoided by obtaining an optimum resin velocity [11] or applying vacuum to the outlet side, which is left for further investigation of the manufacturing parameters beyond this work. Since the number of plies and the component thickness is fixed, increasing the inlet pressure from 3.5 Bar to 7 Bar, which is the standard pressure used at TERMA, allows for an adjustment of the resin velocity.
The voids have not been detectable through COMSOL modelling, thus the simulation of the process is not fully accurate. Otherwise than that, the simulation has proven successful and is deemed sufficiently valid for the purpose of this work.

7.4 Manufacturing of The Spar

Now that the manufacturing of a section of the spar has been simulated satisfactory, the process is expanded to include the entire spar. A model of the spar is made in COMSOL and the input parameters, that are obtained through previous simulations and experiments, are applied.
The objective is to specify the number of in- and outlets in the mold. This is a balancing act between filling time, degree of filling, mold manufacturing costs and mold cleaning time. The work shows that four inlets and three outlets are necessary in order to completely saturate the spar. This requires a total filling time of 28 min, complying with demand 4. Setting the inlet pressure at its maximum of 7 Bars reduces the filling time to 15 min.
An experimental test molding of the entire spar is currently being performed at TERMA, as well as a subsequent estimation of voids in the structure using

a series of internal scan methods. This leaves for an evaluation of the simulation and the double sided mold manufacturing of the spar to be conducted later on.

8. Conclusion

From this work, it is found that the leading edge of a F-35 can be modelled and analysed to obtain realistic results by approximation of the wing geometry and load situation. By evaluation of failure it is concluded that the leading edge will withstand the applied loads, with a index of 0.5. A separate analysis of the core concludes that the honeycomb core material can be replaced by a PMI-foam, in order for the single shot manufacturing to be feasible, complying with demand 1, 2, 5 and 6,

Optimization of the leading edge with respect to stiffness by changing orientation of the composite layup has been successful. A deflection reduction of 3.5% is obtained while still maintaining a low Tsai-Wu failure index.

Work on the investigation of the double sided mold process by the use of CFD simulations and experiments, lead a manufacturing time of 15 minutes the spar complying with demand 4. But as models and simulations are proven accurate for the process with the exception of predicting microscopic voids in the material, such that demand 4, is technically not fulfilled. To fulfill the demand further experimental test on the entire spar is still to be done. It is assumed that a single shot manufacturing is possible for the entire leading edge, but this has not been proven yet, thus demand 3 is not fulfilled.

Acknowledgement

The authors of this work gratefully acknowledge Sintex for sponsoring the 5th MechMan symposium.
The authors would also like to acknowledge TERMA first of all for cooperation with AAU and secondly for providing sheet materials for CFD verification.

References

[1] G. 4.113, "Redesign of the leading edge of the f-35's horizontal stabilizer," technical report, Aalborg University, 2017.

[2] L. C. T. Overgaard, Mechanics of Composite Materials and Structures - Sandwich Structures. Aalborg University, first ed., 2014.

[3] R. M.Jones, Mechanics of Composite Materials. Taylor and Francis, second ed., 1999.

[4] L. C. T. Overgaard, Mechanics of Composite Materials and Structures - Failure Criteria Part 1. Aalborg University, first ed., 2014.

[5] J. S. Arora, Introducution to Optimum Design. Academic Press, fourth ed., 2017.

[6] G. Brown, "Water resources research," Henry Darcy and the making of a law, 2012.

[7] R. L. . J. Kardos, "The permeability and compressibility of aligned and cross ply carbon fiber beds during processing of composites," 2004.

[8] V. A. et. al., "Permeability characterization of stitched carbon fiber preforms by fiber optic sensors," 2011.

[9] M. C. T. Robert S. Pierce, Brian G. Falzon, "Permeability characterization of sheared carbon fiber textile preform," 2016.

[10] A. R. C. Mohamed A. Sohut, "The effect of voids on the flexural fatigue performance of unidirectional carbon fibre composites," 2012.

[11] D. S. R. M. . A. T. Y. Mizutani, "Void formation in an anisotropic woven fiber during resin transfer molding," 18th INTERNATIONAL CONFERENCE ON COMPOSITE MATERIALS, -.